International Geology Review, Vol. 50, 2008, p. 1–16. DOI: 10.2747/0020-6814.50.4.1

Ancient Coastlines in the Continental Shelf of the State of Ceará, Northeast Brazil: Evidence from Sediment Chemistry and Stable Isotopes

WANESSA SOUSA MARQUES,[1] ALCIDES NOBREGA SIAL,[2] ELDEMAR DE ALBUQUERQUE MENOR, VALDEREZ PINTO FERREIRA,

NEG-LABISE, Department of Geology, Federal University of Pernambuco, C.P. 7852, Recife,, Brazil, 50670-000, Brazil

GEORGE SATANDER SÁ FREIRE,

Department of Geology, Federal University of Ceará, C.P. 6011, Fortaleza, Ceará. 60455-970, Brazil

ENJOLRAS DE ALBUQUERQUE MEDEIROS LIMA,

Serviço Geológico do Brasil (CPRM), Avenida Sul, 2291, Afogados, Recife, Brazil, 50770-011

AND ROBERTO LÚCIO BELO DE SOUZA

NEG-LABISE, Department of Geology, Federal University of Pernambuco, C.P. 7852, Recife,, Brazil, 50670-000, Brazil

Abstract

Continental shelf sediments from the state of Ceará, northeastern Brazil, have been studied to investigate meteoric diagenesis of marine sediments of previously defined ancient coastal lines. Major elements for 131 samples of carbonate sediments and C and O isotopes for 51 carapace samples of benthonic foraminifers of the *Amphistegina radiata* and *Peneroplis planatus* species were analyzed. Geochemical signatures of $\delta^{13}C$, $\delta^{18}O$, SiO_2 (stoichiometrically calculated as quartz %), Sr and Mn, and XRD document the impact of meteoric diagenesis on relict sediments from current depths of 25–30 m, 45 m, and 80 m. Morphologies of the marine shelf at these depths, interpreted from previous bathymetric profiles, correspond to holocenic marine terraces. Despite a recent sedimentary cover, it was possible to confirm that these terraces possess relict detrital, biogenic, and continental material, that resulted from erosional reworking of ancient coastlines during the Flandrian transgression.

Introduction

DIAGENETIC CHANGES in biogenic carbonates in general are accompanied by and increase of textural maturity and changes in chemical composition (Hodgson, 1966; Brand and Veizer, 1981; Cícero and Lohmann, 2001). Changes in chemical composition are due to dissolution-reprecipitation in an aqueous medium. Factors that interfere the most in the redistribution of chemical species in carbonates are: (1) the stability of the original carbonate phase; (2) the degree of interaction between carbonate and water (closed system, semi-closed, or open); (3) difference in chemical compositions between seawater and meteoric water; and (4) temperature and salinity of the environment, and vital effects of organisms.

Despite the influence of all these factors, the general tendency of the chemical behavior of the biogenic carbonates, when affected by meteoric diagenesis, point to an increase in the iron and manganese contents and a decrease in strontium and sodium contents (Brand and Veizer, 1981). Concurrently, there is a lowering in the $\delta^{18}O$ and $\delta^{13}C$ values (ibid.; Nagarajan et al., 2008) which are positively correlated in carbonate sediments; these isotopic characteristics suggest subaerial surface exposure (Allan and Matthews, 1982).

Manganese and $\delta^{18}O$ values, in general, show reverse behavior in carbonate samples altered by meteoric diagenesis. This results from the fact that meteoric water is usually pedogenic manganese–enriched and ^{18}O-empoverished (Li et al., 2007). Manganese and strontium values are regarded as good indicators of meteoric diagenesis in carbonates. During the chemical changes that occur along

[1]Corresponding author; email: smarq@yahoo.com.br
[2]Corresponding author; email: sial@ufpe.br

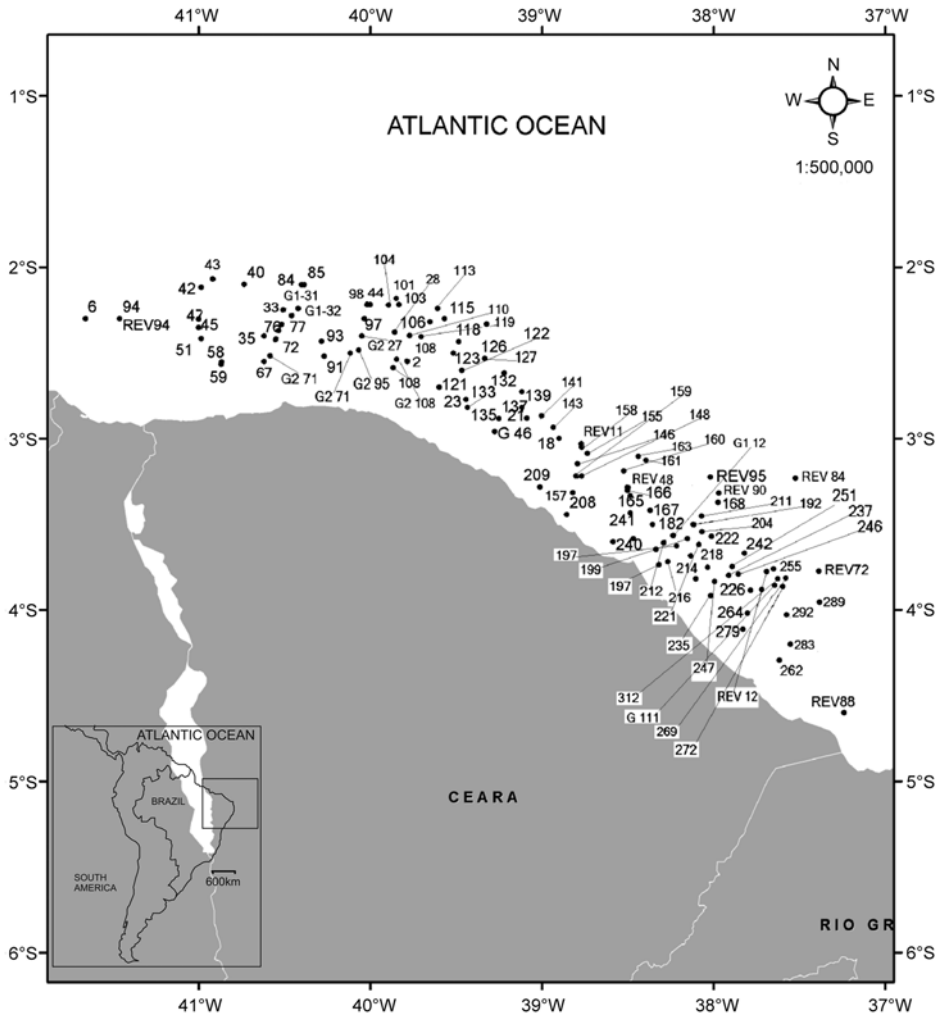

FIG. 1. Location of the study area and of analyzed samples.

with diagenetic stabilization, manganese values tend to increase and strontium values tend to decrease (Brand and Veizer, 1981).

The continental shelf of northeastern Brazil displays ancient coastlines (Manso et. al., 1997), which were constructed during the Flandrian transgression and show relict sediments deposited in mixing zones between sea- and meteoric waters (Freire, 1985). The relict sediments exhibit reworked, ferruginous-stained, quartz grains (França et al. 1976). The ancient coastlines can be inferred from $\delta^{13}C$ and $\delta^{18}O$ values, together with textural characteristics of bottom sediments, including their manganese, strontium, and iron contents and morphological characteristics. The scope of this study is to detect ancient coastlines in the continental shelf of northeastern Brazil by means of major, trace, and stable isotope geochemistry of total sediments, together with indications of bottom morphology from previous studies.

Study Area

The continental shelf of the state of Ceará (Fig. 1) is shallow, has reduced width (60–80 km), moderate gradient (about 1m/km, on average), warm water

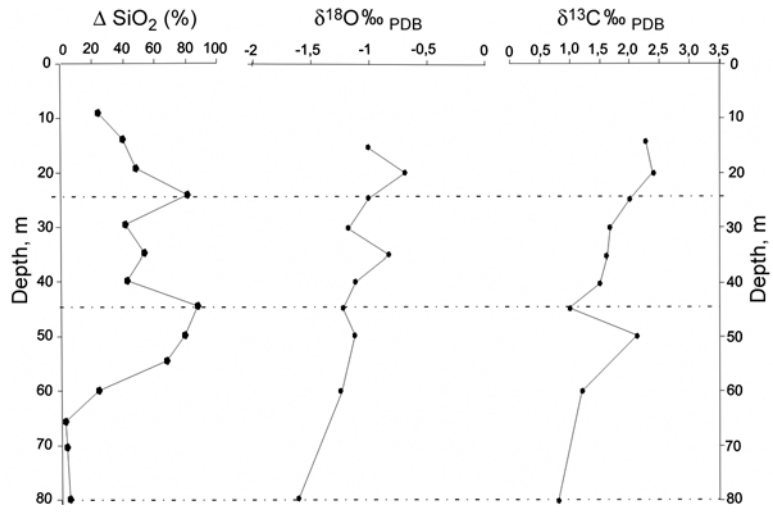

FIG. 2. Variations of Δ SiO_2 (quartz %), $\delta^{18}O$, and $\delta^{13}C$ for sediments from the continental shelf with depth.

(25–30°C), and high salinity (30–38‰) (Summerhayes et al., 1975; Coutinho, 1992; Behling et al., 2000). Its geomorphology includes multiple-step ruptures that correspond to ancient coastlines, a model that is closely associated with sea-level oscillations that occurred since the start of the Flandrian transgression (Freire, 1985). According to Allen (2000), Dabrio et al. (2000), Angulo et al., (2006), Caldas et al. (2006), and Martin et al. (2007), this transgression evolved in a slow and continuous way by transgressive pulses. In the Ceará continental shelf, these steps are more evident at depths of 80 m, between 40 and 50 m, and between 20 and 35 m (Freire, 1985).

The shelf sediments in the study area are constituted by sand and carbonate gravel formed *in situ* and, in lower proportions, by clastic terrigenous provenance and by relict sediments. The carbonate fraction ($CaCO_3$ >75%) predominates beyond 20 m depth in the intermediate and external shelfs, being mainly composed of *Lithothamnium*, *Halimeda*, planktonic and benthonic foraminifers, and mollusks (França et al., 1976; Coutinho, 1992; Behling et al., 2000). Relict sediments are found in larger quantities in the external shelf beyond 40 m depth, and show textural reworking as a main characteristic. The terrigenous fraction includes subrounded quartz grains with shiny, lustreless, or frosted surfaces, sometimes capped (or with fractures filled) by iron oxides (Freire, 1985).

Methods

This study includes a total of 131 bulk chemical analyses of platform sediments grouped in two sets: (1) (Freire, 1985) analyzed samples from Ceará, Brazil collected by dragging during operations of the GEOMAR XVIII-Vitor Hense project (1981) and the GEOMAR XXI-REVISEE project (1983) in the oceanographic ship *Almirante Câmara* of the Brazilian Navy; and (2) a second set from the continental shelf was investigated by the Marine Geology Laboratory (LGMA) of the Federal University of Ceará. The two sets of samples were collected by dragging with a van veen collector (a device constituted by two articulated and open stainless steel shells that lock themselves as they touch the ground, storing sediments in its core).

All samples were washed with deionized water, dried at room temperature, and kept in plastic bags. The initial analytical procedure consisted of homogenization and splitting, and after that an aliquot of each sample was taken for grinding in a porcelain mortar, 100% going through 100-mesh sieve. From each aliquot, 5 g were taken for chemical analysis by X-ray fluorescence (XRF).

The Freire (1985) samples were analyzed by X-ray fluorescence at the Mineral Analyses Laboratory of SUDENE at Recife. For the XRF analysis, the LGMA samples was powdered and were previously dried at 110°C for 6 hours, and next calcined at

TABLE 1. Chemical Analyses of LGMA Samples

Sample	Depth, m	SiO_2	Al_2O_3	Fe_2O_{3t}	MgO	CaO	K_2O	TiO_2	P_2O_5	Mn	Sr	CaO\MgO	Lat (S)	Long (W)
Vh03157	10	68.68	3.00	2.62	1.61	8.46	0.23	2.81	0.04	549	820	5.25	05°45'12''	35°11'12''
Vh03146	15	1.05	0.31	0.16	6.89	43.30	0.04	0.19	0.06	46	2629	6.28	04°52'06''	36°22'48''
Rev88	18	0.00	0.00	0.03	5.97	48.39	0.01	0.03	0.07	16	3052	8.11	04°36'00''	37°14'24''
Vh03147	20	88.31	1.88	0.62	1.02	2.87	0.17	0.56	0.00	158	183	2.81	04°44'30''	36°19'12''
Rev74	20	25.61	0.65	0.05	3.90	34.56	0.18	0.04	0.05	16	3287	8.86	04°56'24''	35°19'30''
Vh03166	20	5.79	0.36	0.07	3.26	45.52	0.10	0.03	0.07	5	5301	13.96	06°45'12''	34°54'30''
G2 96	21	3.20	0.33	0.31	5.90	46.63	0.05	0.01	0.11	30	2940	7.90	02°29'05''	40°04'00''
Vh03171	23	14.63	0.38	0.08	3.90	41.11	0.04	0.02	0.07	18	3588	10.54	06°51'48''	34°46'30''
G2 95	25	9.27	0.60	0.37	5.50	42.85	0.23	0.01	0.10	31	2626	7.79	02°30'06''	40°07'00''
G1 32	25	70.18	3.17	0.47	1.74	12.11	0.90	0.23	0.03	90	1318	6.96	02°17'00''	40°27'30''
G2 71	25	8.53	0.50	0.29	5.42	43.85	0.14	0.02	0.10	36	2611	8.09	02°31'05''	40°35'00''
G2 27	25	12.43	1.39	0.33	4.31	40.56	0.35	0.08	0.09	40	3717	9.41	02°33'05''	39°47'03''
Rev12	25	87.78	1.97	0.25	1.04	3.52	0.22	0.28	0.00	51	217	3.38	03°52'48''	37°43'12''
G1 12	25	7.61	0.25	0.05	3.67	45.38	0.07	0.02	0.10	17	4086	12.37	03°36'30''	38°17'30''
G2 108	28	1.23	0.31	0.34	5.54	48.48	0.03	0.01	0.12	29	2689	8.75	02°35'09''	39°52'00''
Rev95	30	0.12	0.00	0.01	2.78	50.62	0.03	0.01	0.07	5	6482	18.21	03°17'24''	38°00'00''
Vh03134	30	0.67	0.21	0.07	3.86	49.17	0.04	0.02	0.08	14	5200	12.74	04°48'30''	36°37'42''
6	35	0.00	0.00	0.03	5.44	49.13	0.00	0.00	0.08	11	3611	9.03	02°18'00''	41°39'36''
90	35	0.00	0.00	0.02	4.52	50.88	0.00	0.03	0.08	18	4349	11.26	03°28'48''	38°04'48''
G1 31	35	61.05	2.32	0.96	2.21	16.55	0.56	0.12	0.06	111	1550	7.49	02°15'00''	40°30'30''
13	35	61.41	2.81	1.83	2.29	15.69	0.75	0.18	0.06	98	1226	6.85	04°15'00''	36°39'36''
Rev42	35	66.86	2.21	0.18	1.09	14.53	0.68	0.13	0.01	50	3326	13.33	09°06'00''	34°33'36''
89	35	0.39	0.01	0.02	2.78	50.13	0.05	0.01	0.08	16	6060	18.03	03°28'48''	38°04'48''
Rev90	35	0.05	0.05	0.04	3.52	50.58	0.00	0.00	0.08	12	4735	14.37	03°28'48''	38°04'48''
Rev121	35	16.83	1.83	1.55	3.41	36.59	0.28	0.11	0.12	71	3063	10.73	06°48'00''	34°39'36''
Rev72	35	63.70	2.90	0.59	1.58	14.97	0.76	0.08	0.01	53	2981	9.47	03°49'48''	37°22'12''
G 111	38	7.60	0.41	0.15	4.04	42.07	0.11	0.23	0.11	51	3174	10.41	03°54'30''	37°35'00''
Rev52	40	0.00	0.00	0.00	4.48	50.06	0.01	0.00	0.06	5	5133	11.17	05°18'00''	35°24'24''
G 46	40	0.60	0.16	0.16	5.68	49.08	0.00	0.00	0.11	14	2801	8.64	02°57'30''	39°16'30''

Rev75	40	0.15	0.01	0.04	5.47	46.21	0.30	0.00	0.07	15	3839	8.45	03°16'30"	35°06'00"
Rev41	43	0.33	0.03	0.02	3.11	50.42	0.01	0.00	0.07	16	4710	16.21	09°04'48"	35°01'12"
Rev39	55	70.31	2.75	0.15	1.72	12.20	0.73	0.04	0.02	29	2161	7.09	07°28'48"	34°46'48"
Rev48	60	0.03	0.00	0.03	3.19	51.19	0.00	0.00	0.08	18	3165	16.05	03°20'24"	38°40'12"
Rev94	60	0.15	0.00	0.07	4.98	48.19	0.12	0.03	0.12	16	3936	9.68	02°18'00"	41°27'36"
VH3115	60	4.60	0.35	0.05	4.78	46.21	0.14	0.01	0.08	9	3200	9.67	04°15'00"	37°24'30"
94	60	0.58	0.06	0.05	4.45	46.28	0.12	0.02	0.10	30	4314	10.40	02°18'00"	41°27'36"
VH3137	60	2.50	0.45	0.14	3.81	48.13	0.09	0.03	0.10	20	4051	12.63	04°40'00"	36°34'42"
Rev45	60	6.59	0.46	0.32	5.18	44.00	0.09	0.04	0.09	43	2882	8.49	10°36'00"	36°24'00"
VH3153	60	7.83	1.07	1.17	3.85	43.57	0.19	0.06	0.17	76	3063	11.32	05°46'00"	35°00'30"
Rev84	80	0.37	0.02	0.02	5.72	48.26	0.00	0.00	0.08	10	3120	8.44	03°39'36"	38°00'00"
Rev11	80	0.05	0.00	0.03	4.78	49.20	0.00	0.02	0.10	18	3890	10.29	03°01'48"	38°46'12"
VH3126	80	3.46	0.62	0.15	3.11	46.20	0.12	0.03	0.08	22	3888	14.86	04°34'42"	36°53'24"
VH3162	80	3.90	1.76	0.79	4.33	44.26	0.13	0.08	0.10	73	3816	10.22	06°39'42"	34°43'18"

1000°C during a couple of hours in an electrical furnace for determination of loss in ignition. A fused bead was made for each calcined sample, using lithium tetraborate as a flux. The analyses were performed with an XRF unit model Rigaku RIX 3000, equipped with Rh tube, using calibration prepared with international reference material, in LABISE (Stable Isotope Laboratory of Federal University of Pernambuco).

Thirty X-ray diffraction analyses (XRD) of samples of bulk sediments were performed using a Siemens D5000 unit, with KCua emission, scanning of 2 to 45q, under a scan speed of 1I/min. Two samples from each selected depths (10, 15, 20, 25, 30, 35, 40, 45, 50, 55, 60, 65, 70, 75 and 80 meters) have been chosen for XRD analyses. The Mg contents of calcites were calculated from XRD analysis according to Goldsmith and Graf (1958), using the positions (I = 100) of low quartz (3.34 Å) or of aragonite (3.396 Å) for drift correction, and corrected peak measurements of low-Mg or high-Mg calcite.

For C and O isotope analyses, 4 mg of benthonic foraminifer tests from 51 samples of *Amphistegina radiata* and *Peneroplis planatus* species, from the continental shelf were selected. Each sample reacted with orthophosphoric acid for 12 hours, at 25°C. CO_2 released from this reaction was extracted in a conventional high-vacuum extraction line, cryogenically clean, according to Craig's method (1957) and C and O were analyzed in a dual inlet, triple collector SIRA II mass spectrometer, in the stable isotope laboratory (LABISE) of the Department of Geology of the Federal University of Pernambuco. Isotopic compositions were obtained by running CO_2 samples against the Borborema skarn calcite (BSC) reference gas, previously calibrated against NBS-19 and NBS-20, with an analytical precision of 0.1‰, based on multiple analyses of the BSC standard. Results are reported in delta $‰_{PDB}$ notation.

Stoichiometric quartz was calculated from average compositions of kaolinites according to Weaver and Pollard (1973) assuming that kaolinite is the predominating clay mineral in soils of the coastal regions of northeastern Brazil (Summerhayes et. al., 1975). Each $\delta^{13}C$, $\delta^{18}O$ and Δ SiO_2% value plotted in Figure 2 represents the average of five samples.

Results and Discussion

Chemical analyses of 131 samples are presented in Tables 1 and 2. The presence of quartz in shelf sediments is basically due to mechanical dispersion

TABLE 2. Chemical Analyses of Freire (1985) Samples

Sample	Depth, m	SiO_2	Al_2O_3	Fe_2O_3t	MgO	CaO	K_2O	TiO_2	P_2O_5	Mn	Sr	CaO\MgO	Lat (S)	Long (W)
240	10	57.30	0.64	0.07	0.31	13.40	0.41	0.05	0.06	80	2940	43.23	03°48'05"	38°51'06"
241	10	6.60	0.13	0.02	2.00	33.90	0.11	0.02	0.10	48	3600	16.95	03°46'08"	38°48'09"
208	10	3.10	0.29	0.30	3.10	32.80	0.06	0.05	0.16	190	1570	10.58	03°32'05"	38°59'02"
209	10	2.30	0.05	0.02	2.50	35.00	0.04	0.02	0.14	73	2640	14.00	03°33'09"	38°81'07"
197	15	80.70	0.85	0.08	0.43	5.00	0.36	0.04	0.03	140	370	11.63	03°44'07"	38°19'02"
67	18	2.50	0.09	0.06	3.10	33.00	0.10	0.02	0.11	58	2100	10.65	02°33'00"	40°37'09"
58	19	0.51	0.06	0.07	3.00	34.80	0.04	0.01	0.12	65	2650	11.60	02°34'00"	40°52'09"
35	20	77.20	0.42	0.13	0.36	6.80	0.27	0.04	0.07	48	330	18.89	02°24'02"	40°37'07"
279	20	49.30	0.50	0.07	1.00	16.10	0.38	0.06	0.08	180	1100	16.10	04°10'09"	37°40'03"
59	20	0.07	0.07	0.10	3.10	34.30	0.04	0.01	0.13	84	1750	11.06	02°33'09"	40°52'00"
235	22	86.40	0.61	0.10	0.08	3.20	0.39	0.13	0.01	130	630	40.00	03°55'04"	38°01'00"
93	22	1.60	0.07	0.12	2.60	34.80	0.04	0.02	0.12	90	1680	13.38	02°31'06"	40°16'08"
247	22	42.10	0.50	0.04	0.56	19.80	0.41	0.03	0.09	58	3500	35.36	03°55'06"	37°55'05"
108	22	0.97	0.09	0.14	3.50	33.70	0.04	0.02	0.15	83	1760	9.63	02°35'09"	39°52'00"
91	23	57.50	0.66	0.18	0.84	12.40	0.53	0.06	0.10	76	1050	14.76	02°26'00"	40°17'02"
214	23	90.30	0.56	0.07	0.30	1.90	0.32	0.07	0.01	100	210	6.33	03°47'01"	38°11'06"
199	25	91.20	0.56	0.09	0.15	1.50	0.37	0.09	0.11	74	240	10.00	03°43'06"	38°16'00"
2	25	74.50	0.87	0.01	0.28	6.80	0.57	0.14	0.60	145	860	24.29	03°35'05"	38°28'00"
10	25	91.20	0.98	0.11	0.09	0.86	0.57	0.06	0.06	73	160	9.56	03°25'07"	38°42'00"
76	25	51.40	0.29	0.11	0.90	16.40	0.13	0.01	0.09	42	1360	18.22	02°25'06"	40°33'02"
51	25	0.83	0.06	0.04	2.30	35.60	0.04	0.01	0.13	40	2190	15.48	02°25'04"	40°59'05"
157	25	59.90	1.69	0.46	0.84	9.10	0.90	0.19	0.07	190	840	10.83	03°23'02"	38°48'02"
264	27	84.20	0.71	0.06	0.26	3.80	0.41	0.06	0.02	120	520	14.62	04°05'06"	37°49'04"
262	28	5.10	0.09	0.02	0.57	36.40	0.06	0.02	0.08	25	6310	63.86	04°01'09"	37°48'04"
75	30	0.85	0.07	0.06	3.60	33.60	0.04	0.02	0.11	76	2300	9.33	02°26'00"	40°33'04"
77	30	0.82	0.08	0.05	3.50	33.20	0.05	0.02	0.10	31	2650	9.49	02°22'08"	40°32'04"
135	30	53.20	0.53	0.21	1.30	15.10	0.39	0.07	0.09	160	850	11.62	02°56'00"	39°26'00"
182	30	76.20	0.56	0.05	0.27	6.90	0.45	0.05	0.03	48	1330	25.56	03°34'01"	38°14'05"

276	30	81.60	0.74	0.11	0.28	4.40	0.49	0.15	0.03	210	600	15.71	04°05'03''	37°43'01''
277	30	82.30	0.66	0.07	0.26	4.60	0.45	0.05	0.02	94	640	17.69	04°05'09''	37°43'09''
155	30	85.80	1.06	0.13	0.14	2.50	0.70	0.13	0.02	83	219	17.86	03°13'03''	38°48'05''
148	30	75.70	0.82	0.11	0.50	6.10	0.57	0.03	0.04	62	420	12.20	03°19'01''	38°49'08''
237	30	87.50	0.64	0.07	0.17	2.60	0.45	0.07	0.02	90	420	15.29	03°52'00''	37°56'01''
251	30	37.40	0.29	0.04	1.20	21.40	0.23	0.02	0.10	28	2370	17.83	03°53'09''	37°47'00''
272	30	82.70	0.71	0.05	0.26	4.30	0.53	0.03	0.03	120	480	16.54	03°59'04''	37°38'09''
283	30	1.00	0.04	0.02	3.20	33.90	0.04	0.02	0.14	15	2540	10.59	04°12'00''	37°33'04''
289	30	31.30	0.34	0.02	0.48	24.00	0.30	0.02	0.10	32	4650	50.00	04°16'05''	37°25'02''
274	33	34.80	0.48	0.05	0.35	21.80	0.37	0.04	0.09	32	4640	62.29	04°01'01''	37°40'00''
159	33	67.30	0.42	0.06	0.59	10.60	0.34	0.03	0.06	10	1030	17.97	03°20'03''	38°41'07''
246	33	59.00	0.69	0.07	0.24	12.80	0.49	0.06	0.05	120	3460	53.33	03°51'01''	37°53'04''
255	35	28.50	0.32	0.06	1.40	25.10	0.23	0.04	0.13	170	2250	17.93	03°49'04''	37°40'08''
97	35	50.20	0.50	0.18	1.30	15.70	0.36	0.04	0.11	150	850	12.08	02°24'00''	40°03'01''
165	35	88.50	0.64	0.08	0.16	2.40	0.49	0.08	0.02	62	300	15.00	03°26'07''	38°29'07''
167	35	90.80	0.71	0.08	0.13	1.30	0.45	0.07	0.02	52	220	10.00	03°29'07''	38°22'08''
218	35	91.50	0.64	0.05	0.04	1.40	0.49	0.05	0.02	54	250	35.00	03°45'05''	38°02'00''
23	36	1.00	0.08	0.08	3.70	33.50	0.04	0.15	0.13	85	2450	9.05	02°49'04''	39°26'00''
28	36	0.52	0.06	0.04	2.90	34.60	0.04	0.01	0.13	53	2100	11.93	02°30'07''	39°51'04''
106	37	0.38	0.05	0.02	3.90	33.40	0.07	0.01	0.12	32	1850	8.56	02°25'00''	39°51'00''
121	37	3.30	0.14	0.08	3.30	33.10	0.05	0.03	0.13	100	2500	10.03	02°42'02''	39°36'00''
136	38	52.10	0.48	0.25	1.20	15.80	0.32	0.04	0.10	150	940	13.17	02°55'00''	3920'04''
4	38	8.50	0.09	0.03	0.26	32.00	0.14	0.01	0.11	10	5310	123.08	03°23'07''	38°24'00''
33	38	79.00	0.82	0.13	0.32	5.40	0.53	0.05	0.09	78	360	16.88	02°20'00''	40°31'03''
110	38	0.75	0.07	0.04	3.70	33.60	0.04	0.02	0.15	40	1880	9.08	02°30'06''	39°47'00''
47	38	0.76	0.06	0.04	2.10	35.70	0.04	0.01	0.12	26	2400	17.00	02°21'08''	41°00'03''
122	39	52.00	0.34	0.06	0.66	17.40	0.25	0.02	0.08	100	1650	26.36	02°39'03''	39°32'02''
158	39	85.40	1.19	0.15	0.23	2.40	0.74	0.09	0.03	86	290	10.43	03°13'03''	38°46'06''
330	40	32.40	0.42	0.05	1.20	22.40	0.38	0.02	0.09	140	3180	18.67	04°21'03''	37°17'01''
5	40	2.30	0.03	0.02	1.20	36.10	0.04	0.01	0.12	10	2450	30.08	03°18'00''	38°22'07''
123	40	1.50	0.05	0.02	2.70	35.10	0.04	0.02	0.12	52	2450	13.00	02°36'07''	39°28'05''

Table continues

Sample	Depth, m	SiO_2	Al_2O_3	Fe_2O_3t	MgO	CaO	K_2O	TiO_2	P_2O_5	Mn	Sr	CaO\MgO	Lat (S)	Long (W)
98	40	52.40	0.40	0.13	0.84	16.10	0.28	0.01	0.08	120	1550	19.17	02°18'05''	40°02'02''
132	40	65.30	0.50	0.04	0.84	11.20	0.37	0.01	0.06	52	670	13.33	02°44'03''	39°19'00''
133	40	64.70	0.37	0.10	0.78	11.30	0.18	0.04	0.07	120	820	14.49	02°48'07''	39°21'02''
137	40	58.00	0.45	0.09	1.10	14.20	0.27	0.02	0.08	130	880	12.91	02°53'00''	39°15'06''
160	40	24.80	0.18	0.07	1.90	25.80	0.16	0.03	0.13	34	1840	13.58	03°17'08''	38°30'00''
212	40	92.60	0.56	0.07	0.14	0.86	0.41	0.07	0.01	150	200	6.14	03°41'05''	38°08'00''
216	40	91.30	0.64	0.07	0.11	1.40	0.45	0.07	0.01	60	310	12.73	03°49'04''	38°07'03''
222	40	76.80	0.90	0.07	0.26	6.00	0.70	0.04	0.03	150	990	23.08	03°41'01''	37°55'03''
292	40	71.80	0.74	0.07	0.32	8.50	0.57	0.04	0.04	130	1590	26.56	04°07'07''	37°35'04''
293	40	21.30	0.56	0.07	0.72	21.30	0.45	0.05	0.10	90	3870	29.58	04°06'00''	37°37'09''
336	43	2.00	0.05	0.02	1.30	37.20	0.04	0.02	0.09	21	4100	28.62	04°37'08''	37°09'05''
146	45	86.80	0.85	0.12	0.23	2.60	0.49	0.04	0.02	92	240	11.30	03°13'07''	38°53'08''
204	45	89.90	0.82	0.08	0.11	1.60	0.53	0.05	0.01	120	210	14.55	03°38'02''	38°05'04''
269	50	86.20	0.79	0.06	0.13	2.50	0.60	0.06	0.02	43	270	19.23	03°56'02''	37°39'05''
161	50	20.90	0.45	0.07	1.50	27.43	0.35	0.05	0.13	64	2600	18.29	03°15'02''	38°33'09''
221	50	88.70	0.58	0.07	0.26	2.30	0.45	0.04	0.01	69	230	8.85	03°43'00''	37°58'02''
166	50	91.10	0.74	0.09	0.08	1.10	0.53	0.06	0.02	50	230	13.75	03°25'05''	38°22'07''
168	55	70.80	0.82	0.08	0.41	7.90	0.66	0.06	0.04	86	1120	19.27	03°29'03''	38°12'05''
45	58	0.52	0.05	0.03	2.40	35.50	0.04	0.01	0.13	23	2090	14.79	02°18'08''	41°00'02''
192	60	85.70	0.79	0.07	0.23	3.00	0.62	0.04	0.02	100	320	13.04	03°35'02''	38°09'08''
8	60	92.20	0.77	0.07	0.06	0.65	0.49	0.06	0.12	62	170	10.83	03°18'08''	38°30'06''
211	60	88.50	0.74	0.05	0.05	2.40	0.57	0.03	0.01	33	430	48.00	03°37'03''	38°05'09''
21	60	13.50	0.34	0.14	2.80	28.60	0.13	0.06	0.13	130	2740	10.21	02°56'08''	39°13'03''
119	60	7.00	0.11	0.02	2.94	31.60	0.14	0.02	0.17	52	2420	10.75	02°30'05''	39°31'00''
164	60	25.00	0.32	0.08	1.40	26.70	0.27	0.06	0.13	86	2250	19.07	03°20'07''	38°29'04''
163	65	3.10	0.08	0.05	1.90	35.80	0.05	0.02	0.14	65	2900	18.84	03°15'03''	38°29'03''
43	70	2.90	0.08	0.04	1.80	35.40	0.04	0.02	0.13	60	1850	19.67	02°07'04''	40°59'07''
18	80	3.10	0.08	0.04	1.10	35.00	0.09	0.01	0.14	50	1810	31.82	03°00'00''	38°54'02''
127	80	12.40	0.16	0.04	2.60	28.90	0.18	0.04	0.34	180	1630	11.12	02°37'01''	39°13'07''

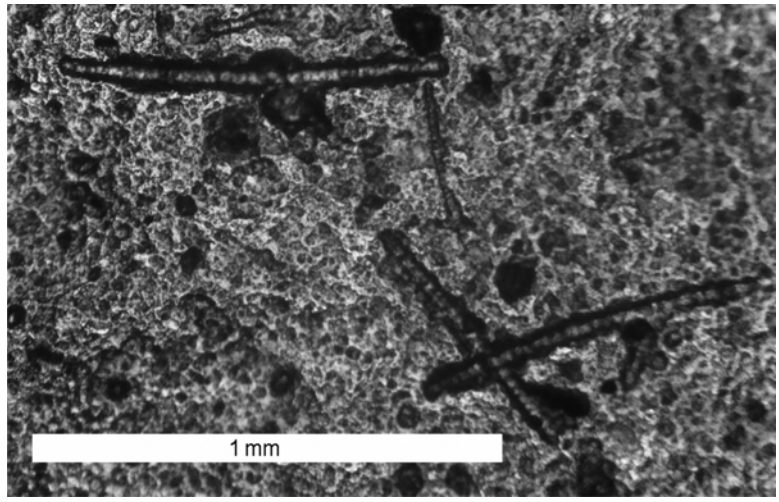

FIG. 3. Spicules of siliceous organisms in residual material from sample VH-3126 (80 m depth) after etching with 10% N HCl. Observation under LN/40× magnification.

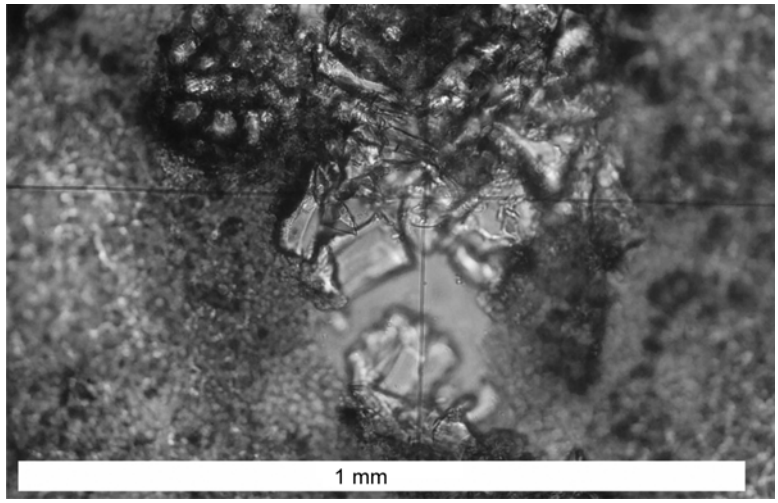

FIG. 4. Angular quartz grains in residual material from sample VH-3126 (80 m depth) after etching with 10% N HCL. Observation under LN/200× magnification).

of this mineral through fluvial plumes, or to sea water abrasion directly on the coast; eolian transport provides an accessory contribution. Although eolian transport may reach considerable distances, its origin can be defined by morphoscopic analysis of the grains (Timireva and Velichko, 2006).

Normally, the concentration and dimension of quartz grains in shelf sediments rapidly decrease oceanward. However, in the Ceará continental shelf, quartz sands (quartz ≥80%) are found at depths of 25 m and 45 m (Fig. 2), coinciding with geomorphological marks recognized by Freire (1985). At depths beyond 25 m, the presence of quartz rapidly decreases, considering samples chemically analyzed in this study. Beyond 65 m depths, the presence of quartz is merely accessory (< 2%), passing to 3% at 80 meters. In this external portion of the shelf, the presence of quartz corresponds mainly to

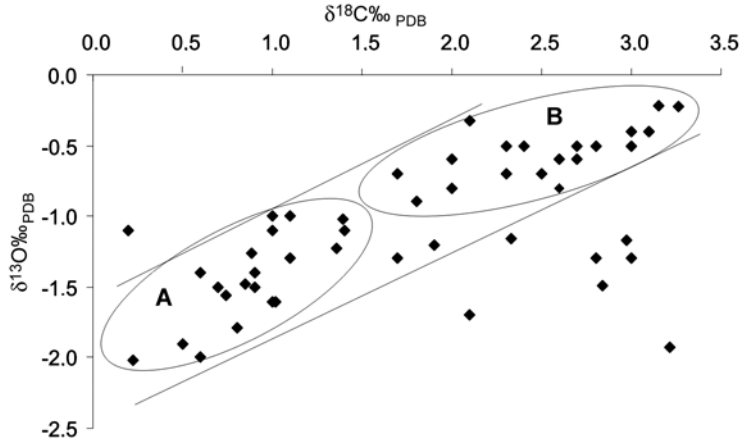

FIG. 5. Scatter diagram of $\delta^{18}O$ versus $\delta^{13}C$. Isotopic A and B clusters for carbonates of benthonic species: *Amphistegina radiata* and *Peneroplis planatus*.

the biogenic contribution of spicules of siliceous organisms sedimented on the submarine floor, as well as grains transported by the wind (Figs. 3 and 4).

The difficulty of locating sedimentary records of geomorphological marks of ancient coastlines (e.g. 20,000 BP) has as an obstacle a possible total covering of these records by subsequent sedimentation, particularly if sedimentation rates are elevated in the shelf under consideration. In fact, even under a regional sedimentation rate of 14 cm/1000 years, defined by Behling et al. (2000) for marine shelves in northeastern Brazil, these features would be today covered by almost 3 meters of more recent sediments. However, a small inflection in the variation curve of quartz % is present at 80 m depth, influenced by one sample (no. 127) with important participation of this mineral (12%). In another samples that have not been chemically analyzed (e.g. sample GI-29), expressive presence of quartz at 80 m depth has been detected by XRD. These are meaningful data and suggest that, with some luck, sample dredging at this depth level can spot well-exposed, under-exposed, or reworked zones of ancient coastlines.

Isotope data are presented in Table 3. The general behavior of $\delta^{18}O$ shows average values decreasing from 15 to 80 m depths (Fig. 2). This, in principle, indicates a cooling of water with depth, a phenomenon amply recognized in oceanography (Chester, 2000) and, in the present case, well-registered isotopically in carbonates of carapaces of benthonic species *Amphistegina radiata* and *Peneroplis planatus*. Inasmuch as $\delta^{18}O$ values also reflect the influence of mixing of continental water (^{16}O-enriched) in marine environments (Li et.al., 2007), minor inflections at 30 and 45 m depths display average $\delta^{18}O$ values that are slightly lower, suggesting relicts of benthonic species at these levels. These $\delta^{18}O$ values may have resulted from meteoric diagenesis which, according to Brand and Veizer (1981), tend to decrease.

Likewise, $\delta^{13}C$ values decrease, in a general way, from 15 m to 80 m depths, with a lower average value at 45 m depth, followed by an increase at the 50 m depth, then reaching a minimum value at a depth of 80 m. The $\delta^{13}C$ values do not always accompany those of $\delta^{18}O$ in cases of meteoric diagenesis, because meteoric waters are not derived uniquely from soils (Brand and Veizer, 1981).

The isotope behavior faces a duality of interpretation: (a) for $\delta^{18}O$, water temperature and influence of continental water; (b) for $\delta^{13}C$, organic productivity and continental water influx. Interpretation can become more complicated if present-day sediments were mixed with relict carbonate sediments. Even so, a positive correlation exists between $\delta^{18}O$ and $\delta^{13}C$ values (Fig. 5), and two groups of isotope behavior are distinguished if the benthonic species are considered: (A) carbonates from benthonic foraminifers, with influence of continental waters; and (B) carbonates from benthonic foraminifers, with influence of water temperature.

TABLE 3. Results of Isotope Analyses in Carbonate Sediments

Sample	G1 38	G1 39	rev91	Vh 3115	G2 109	2 93	G2 68	G2 70	2 94	G1 40	1 35	G1 36	G1 34	rev86	G2 20	G2 96
Depth(m)	14	15	15	15	16	16	17	17	17	18	18	18	19	20	21	21
$\delta^{18}O‰_{PDB}$	–0.8	–0.9	–2.0	–1.9	–1.7	–0.3	–0.7	–0.4	–0.5	–0.7	–0.4	–0.6	–0.5	–1.8	–0.6	–0.4
$\delta^{13}C‰_{PDB}$	2.6	1.8	0.2	3.2	2.1	3.2	2.5	3.1	2.7	2.3	3.1	2.7	2.4	0.8	2.6	3.1

Sample	G2 105	rev106	G-115	Vh03134	6	90	G1 31	13	89	G2 104	Rev41	93	rev 09	rev 07	vh17	g2-46
Depth(m)	30	30	30	30	35	35	35	35	35	40	43	45	45	50	50	50
$\delta^{18}O‰_{PDB}$	–1.5	–1.6	–1.3	–2	–1	–0.7	–0.5	–0.6	–1.1	–1.1	–1.3	–1.4	–1.2	–1.0	–1.2	–1.2
$\delta^{13}C‰_{PDB}$	0.7	1.0	0.9	0.6	1	1.7	2.3	2	1	1.4	1.7	0.6	1.4	1.4	2.3	3.0

Sample	G1 32	G2 71	G2 27	G2 21	rev93	G1 25	G1 33	G2 108	94	VH3137	Rev45	Rev84	Rev11	5	rev44	G2 95
Depth(m)	25	25	25	25	25	28	28	28	60	60	60	80	80	30	30	25
$\delta^{18}O‰_{PDB}$	–0.5	–0.3	–1.2	–1.5	–1.5	–0.5	–0.3	–0.8	–1.1	–1.4	–1.3	–1.9	–1.3	–1.6	–1.5	–0.4
$\delta^{13}C‰_{PDB}$	3	2.1	1.9	0.9	0.9	2.8	3.3	2	0.2	0.9	3	0.5	1.1	0.7	2.8	3

Sample	Rev48	VH3115	VH 3171
Depth(m)	60	60	23
$\delta^{18}O‰_{PDB}$	–1	–1.9	–1,3
$\delta^{13}C‰_{PDB}$	1.1	3.2	2,8

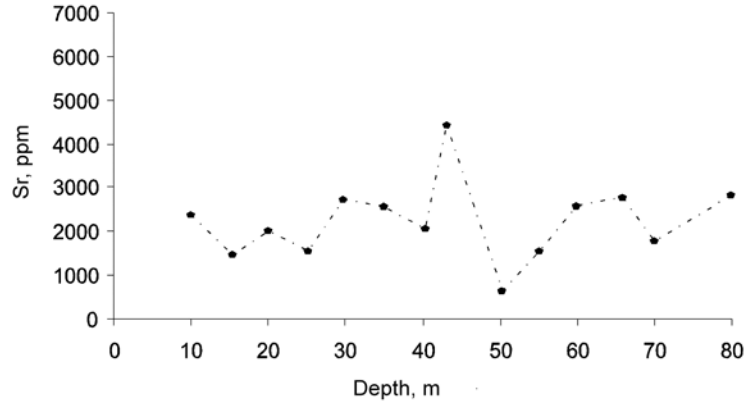

FIG. 6. Variation of average Sr contents in continental shelf carbonate sediments.

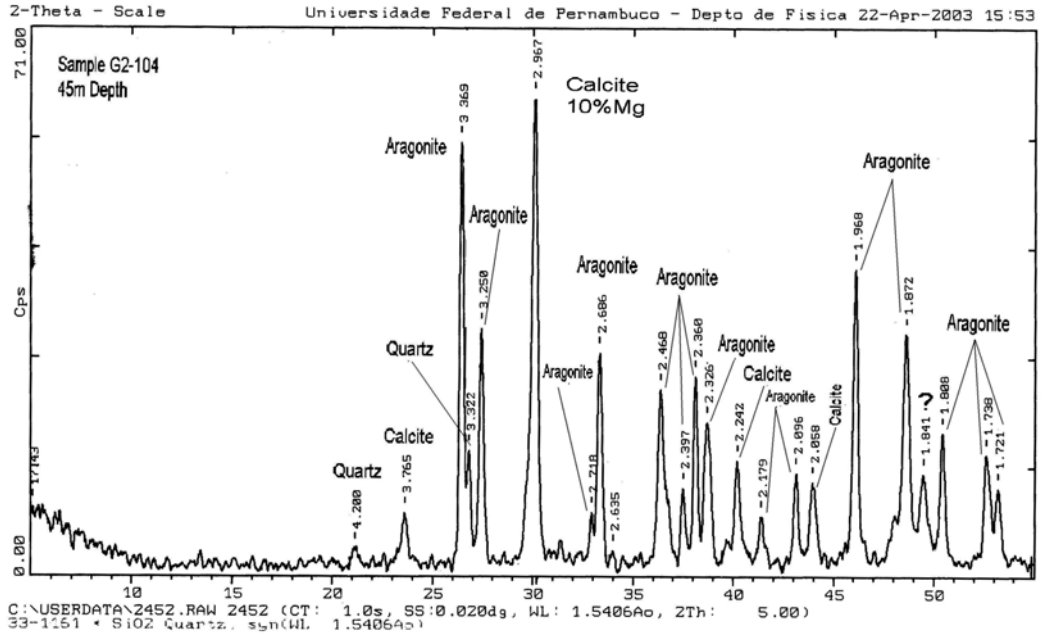

FIG. 7. X-ray difractogram for sample G2-104 (45 m depth).

Group A is characterized by lower $\delta^{13}C$ values (< 1.5‰), resulting from mixing with continental waters, confirmed by lower $\delta^{18}O$ values (< –1‰). This group reflects marine sedimentation environments with strong evidence of continentality. High $\delta^{13}C$ values of biogenic carbonates imply high biological productivity (Wynn and Read, 2007) and vice-versa. In the case of group A, its lower productivity is related to restrictive factors of continental waters such as excessive turbidity that limits photosynthetic reactions. Group B is characterized by higher $\delta^{13}C$ values (> 1.5 ‰) and $\delta^{18}O$ (> –1‰) as a result of the association of high temperature and productivity.

Regarding the behavior of strontium, its concentration coefficient is high in carbonate minerals,

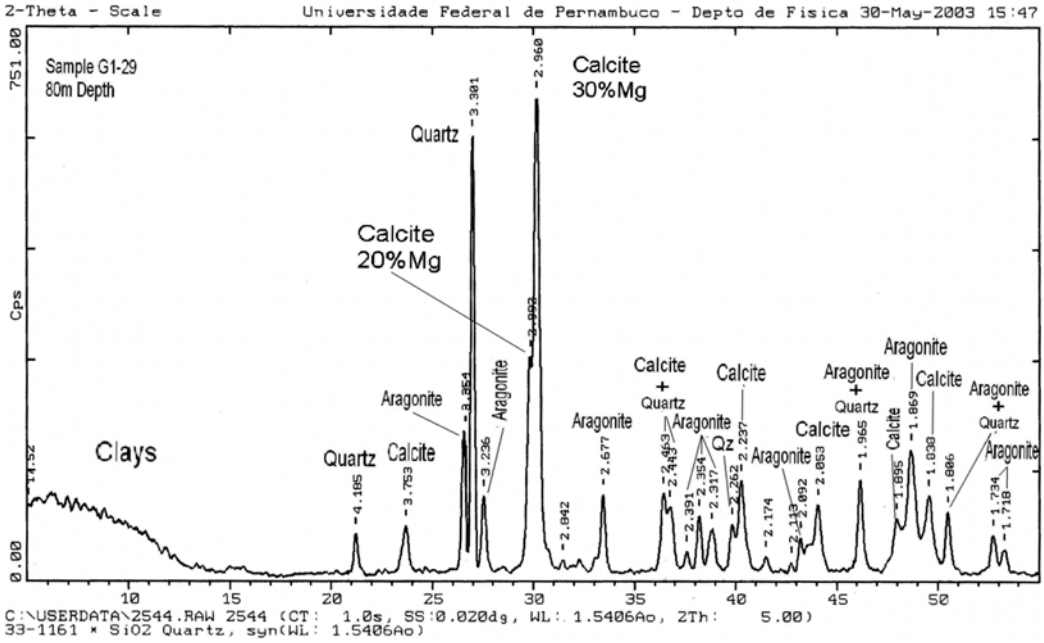

FIG. 8. X-ray diffractogram for sample GI-29 (80 m depth).

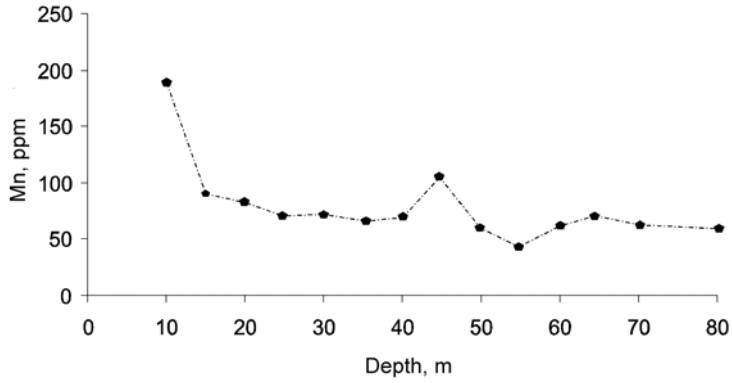

FIG. 9. Variation of Mn contents in continental shelf carbonate sediments.

especially in aragonite, where values between 6,000 and 10,000 ppm may be reached (Tucker and Wright, 1990). In carbonate sediments of the continental shelf of the state of Ceará, Sr average values vary from 500 to 4,500 ppm. In these sediments, the paragenesis of carbonate minerals include, besides aragonite, low-Mg calcite and high-Mg calcite (Mg diadochy in the order of 20 to 30%). Higher Sr contents are usually an indication of predominant or an important aragonite fraction in the bulk sediment, likely a consequence of mineralogically preserved phyla typified by this metastable form of calcium carbonate. Among these phyla figure species that have shallow-water habitat as *Halimeda*, an abundant alga in this area of study, but not essentially an indicator of marine terraces. In any event, the highest average Sr content is observed at 45 m depth (Fig. 6) and, in fact according to XRD analyses,

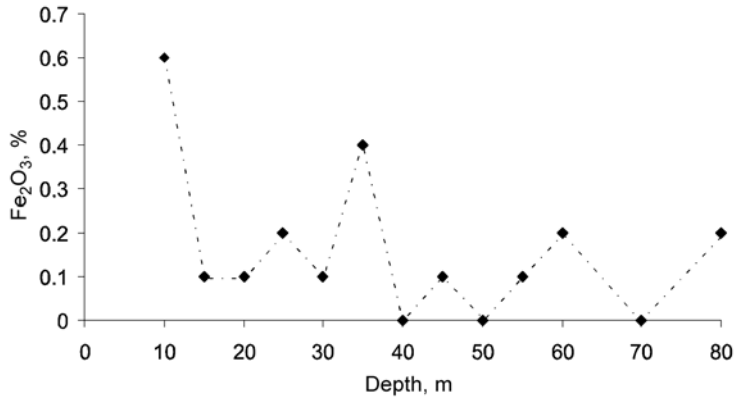

FIG. 10. Variation of average Fe_2O_3 contents in continental shelf carbonate sediments.

aragonite is relatively abundant at this depth level (Fig. 7).

Subordinate aragonite occurs at depths beyond 60 m associated with low or high Mg-calcites, and at 80 m, with the presence of quartz (Fig. 8). In this case, the paragenesis suggests mixing of biota, likely non-contemporaneous, and the possibility of reworked detrital quartz material, remaining from ancient coastal terraces.

Regarding manganese, average contents are markedly more elevated (190 ppm) at 10 m depth (Fig. 9) that corresponds to the influx of pedogenic particules and sedimentation of this chemical species through riverine influxes. Toward the ocean, Mn concentrations rapidly decrease and stabilize around approximately 70 ppm, with a slight decrease to 60 ppm in the isobaths of 70–80 m. Apparently, Mn contents of the studied shelf sediments do not delimit Flandrian coastal terraces, except at the 45 m depth, where an enrichment factor has elevated its average concentration to 110 ppm. In this case, the 45 m depth is distinguished by more elevated Sr and Mn average values, and not by divergent values, as pointed out by Brand and Veizer (1981) for cases in which meteoric diagenesis occurs. This divergence is due to the fact that, with the evolution of the Flandrian transgression, the coastal terrace of the time, which is now 45 m deep, underwent a process of sedimentary accumulation with differentiated physical-chemical conditions thus causing overlapping of sediments deposited under different geochemical conditions. There is, in consequence, an accumulation of biogenic carbonates, with strong presence of aragonite (Sr-enriched carbonate) in the middle and external portions of the continental shelf.

Iron oxide average content (Fig. 10), and likewise manganese, presents a marked value at 10 m depth (0.6% Fe_2O_3) that, by its identical provenance, resulted from the contemporaneous influx of continental pedogenic sediments. Considering a 0.1% Fe_2O_3 background, several depth levels (25, 35, 45, 60, and 80 m) display Fe -enrichment, calling attention to the 35 m depth (0.4% Fe_2O_3). In the Fe_2O_3 vs. depth distribution diagram (Fig. 10), the jigsaw behavior of the Fe_2O_3 curve results from mechanical scattering along the shelf, more widespread than for manganese.

Conclusions

Meteoric diagenesis has been documented in bottom sediments of the continental shelf of northeastern Brazil at depths where relict sediments correspond to reworking of holocenic coastlines: 20–25 m, 45 m, and 80 m. Evidence includes, at these depth levels, more elevated average silica-free contents (quartz %), Mn and Fe, in total sediment, associated with lower $\delta^{13}C$ and $\delta^{18}O$ values in carbonate carapaces of benthonic foraminifers of *Amphistegina radiata* and *Peneroplis planatus*. Associated with these geochemical features, a paragenesis of Mg-calcites with distinct degrees of Ca^{++} for Mg^{++} diadochy, is associated particularly with bathymetric domains between 70 and 80 m. The combination of all these geochemical and mineralogical parameters is incomplete, due to mixing of contemporaneous and relict sediments, under distinct environmental

conditions in relation to the latter, due to the former being formed during the Flandrian transgression, still in progress today.

Acknowledgments

We express our gratitude to Gilsa M. Santana and Vilma S. Bezerra for assistance with the stable isotope analyses in this study. Thanks are also due to LGMA for cession of some samples used in this study. Finally thanks are extended to CAPES for a scholarship granted to WSM. This is NEG-LABISE contribution No. 250.

REFERENCES

Angulo, R. J., Lessa, G. C., and Souza, M. C., 2006, A critical review of mid- to late-Holocene sea-level fluctuations on the eastern Brazilian coastline: Quaternary Science Reviews, v. 25, p. 486–506.

Allan, J. R., and Mattews, R. K., 1982, Isotope signatures associated with early meteoric diagenesis. Sedimentology, v. 29, p. 797–817.

Allen, J. R. L., 2000, Late Flandrian (Holocene) tidal palaeochannels, Gwent Levels (Severn Estuary), SW Britain: Character, evolution, and relation to shore: Marine Geology, v. 162, p. 353–380.

Behling, H., Arz, W. H., Pätzold, J., and Wefer, G., 2000, Late quaternary vegetational and climate dynamics in northeastern Brazil: Inferences from marine core GeoB3104-1: Quaternary Science Reviews, v. 19, p. 981–994.

Brand, U., and Veizer, J., 1981, Chemical diagenesis of a multicomponent carbonate system–2: Stable isotopes: Journal of Sedimentary Petrology, v. 51, p. 987–997.

Caldas, L. H. O., Stattegger, K., and Vital, H., 2006, Holocene sea-level history: Evidence from coastal sediments of the northern Rio Grande do Norte coast, NE Brazil: Marine Geology, v. 228, p. 39–53.

Chester, R., 2000, Marine geochemistry: London, UK, Blackwell Scientific, 491 p.

Cícero, A. D., and Lohmann, K. C., 2001, Sr/Mg variation during rock-water interaction: Implications for secular changes in the elemental chemistry of ancient seawater: Geochimica et Cosmochimica Acta, v. 65, p. 741–761.

Coutinho, P. N., 1992, Sedimentos carbonáticos da plataforma continental brasileira: Revista de Geologia UFC, Fortaleza, v. 6, p. 65–73.

Craig, H., 1957, Isotope standard for carbon and oxygen and correction factors for mass spectrometry analysis of carbon dioxide: Geochimica et Cosmochimica Acta, v. 12, p. 133–149.

Dabrio, C. J., Zazo, C., Goy, J. L., Sierro, F. J., Borja, F., Lario, J., González, J. A., and Flores, J. A., 2000., Depositional history of estuarine infill during the last postglacial transgression (Gulf of Cadiz, Southern Spain): Marine Geology, v. 162, p. 381–404.

França, A. M. C., Coutinho, P. N., and Summerhayes, C. P., 1976, Sedimentos superficiais da margem continental nordeste brasileira: Revista Brasileira de Geociências. v. 6, p. 71–88.

Freire, G. S. S., 1985, Geologia marinha da plataforma continental do Ceará: Unpubl. Master's dissertation in Geosciences, Universidade Federal de Pernambuco-UFPE, Recife, 132 p.

Goldsmith, J. R., and Graf, D. L., 1958, Relations between lattice constants and compositions of the Ca-Mg carbonates: American Mineralogist, v. 43, p. 84–101.

Hodgson, W. A., 1966, Carbon and oxygen isotope ratios in diagenetic carbonates from marine sediments: Geochimica et Cosmochimica Acta, v. 30, p. 1223–1233.

Li, J. W., Vasconcelos, P., Duzgoren, A. N., Yan, D. R., Zhang, W., Deng, X. D., Zhao, X. F., Zeng, Z. P., and Hu, M. A., 2007, Neogene weathering and supergene manganese enrichment in subtropical South China: An $^{40}Ar/^{39}Ar$ approach and paleoclimatic significance: Earth and Planetary Science Letters, v. 256, p. 389–402.

Manso, V. A. V., Corrêa, I. C. S., Barros, C. E., and Baitelli, R., 1997, Sedimentologia da Plataforma Continental entre Aracaju (SE) e Maceió (AL): Anais da Academia Brasileira de Ciências, v. 69, p. 505–520.

Martin, R. E., Leorri, E., and McLaughlin, P. P., 2007, Holocene sea level and climate change in the Black Sea: Multiple marine incursions related to freshwater discharge events: Quaternary International, v. 167/168, p. 61–72.

Nagarajan, R., Sial, A. N., Altrin, J. S. A., Madhavaraju, J., and Nagendra, R., 2008, Carbon and oxygen isotope geochemistry of Neoproterozoic limestones of the Shahabad Formation, Bhima basin, Karnataka, southern India: Revista Mexicana de Ciências Geológicas, v. 25, no. 2, p. 225–235.

Summerhayes, C. P., Coutinho A. P. N., França, M. C., and Ellis, J. P., 1975, Upper continental margin sedimentation of Brazil: Contributions to Sedimentology, v. 4, p. 44–78.

Timireva, S. N., and Velichko, A. A., 2006, Depositional environments of the Pleistocene loess-soil series inferred from sand grain morphoscope—a case study of the East European Plain: Quaternary International, v. 152/153, p. 136–145.

Tucker, M. E., and Wright, V. P., 1990, Carbonate sedimentology: London, UK, Blackwell Scientific, 421 p.

Weaver, C. E., and Pollard, L. D., 1973, The chemistry of clay minerals. Amsterdam, The Netherlands, Elsevier, Developments in Sedimentology, v. 15, 187 p.

Wynn, T. C., and Read, J. F., 2007, Carbon–oxygen isotope signal of Mississippian slope carbonates, Appalachians, USA: A complex response to climate-driven fourth-order glacio-eustasy: Palaeogeography, Palaeoclimatology, Palaeoecology, v. 256, p. 254–272.